Chapter 5

Geochemistry: Elements

Michael D. Glascock and Robert J. Speakman

As part of the study of metavolcanic and metasedimentary rocks found in the Carolina Slate Belt, 80 samples were submitted to the Archaeometry Laboratory at the University of Missouri Research Reactor Center (MURR) for chemical analysis. The goal was to determine the range of variability in the elemental composition of these rocks.

The samples included 71 rock specimens obtained from the 12 quarry zones surrounding Fort Bragg and nine Savannah River projectile points found at Fort Bragg itself (see Appendix A). Three different methods were used to measure the concentrations of elements within these samples: instrumental neutron activation analysis (NAA), x-ray fluorescence spectrometry (XRF), and inductively coupled plasma mass spectrometry (ICP-MS).

In this chapter, we briefly review the analytical methods used for determining composition, describe the quantitative methods used to examine the elemental data set, and statistically identify a number of compositional groups that correspond to the quarry zones described in previous chapters.

Analytical Methods

The rock samples and artifacts were ground into powders at the University of North Carolina at Chapel Hill using an aluminum-oxide shatter box. The samples were then shipped to MURR in powdered form. The original sample material was subdivided into aliquots of 350 mg for NAA, 150 mg for ICP-MS, and the remainder (typically 2.5 g) for XRF. The details of our analytical procedures are presented in Appendixes D-F, along with complete tabulations of the data. Here we provide only a brief overview of each method.

NAA is perhaps the most widely used method in archaeological provenance studies. It involves bombarding the samples with neutrons in a nuclear reactor and then measuring the gamma radiation emitted by these samples. The gamma counts can be used to derive very precise estimates of the concentrations of various elements present. A protocol involving two irradiations and three counts yielded data on a total of 33 elements: Al (aluminum), Ba (barium), Ca (calcium), Dy (dysprosium), K (potassium), Mn (manganese), Na (sodium), Ti (titanium), V (vanadium), As (arsenic), La (lanthanum), Lu (lutetium), Nd (neodymium), Sm (samarium), U (uranium), Yb (ytterbium), Ce (cerium), Co (cobalt), Cr (chromium), Cs (cesium), Eu (europium), Fe (iron), Hf (hafnium), Ni (nickel), Rb (rubidium), Sb (antimony), Sc (scandium), Sr (strontium), Ta (tantalum), Tb (terbium), Th (thorium), Zn (zinc), and Zr (zirconium). These data were tabulated in parts per million (Appendix D).

XRF has also been widely used to determine the chemical composition of rocks. The sample is bombarded with x-rays, and the secondary x-rays emitted by the sample are measured to estimate the elements that are present. These measurements resulted in data for 21 elements, namely Na, Mg (magnesium), Al, Si (silicon), K, Ca, Ti, Mn, Fe, Cu (copper), Zn, Ga (gallium), Rb, Sr, Y (yttrium), Zr, Nb (niobium), Ba, Pb (lead), Th, and U. In accordance with geological convention, the major elements were converted to percent oxides and the trace elements are listed in parts per million (Appendix E).

ICP-MS is a very sensitive method capable of measuring many elements, including some that cannot be detected by NAA. The method works by injecting the sample, often in dissolved form, into a chamber containing an extremely hot gas (plasma). In this ultra-hot environment, the molecules in the sample are broken down into charged atoms that can be identified and counted with a mass spectrometer. Data were obtained for the 14 rare earths: La, Ce, Pr (praseodymium), Nd, Sm, Eu, Gd (gadolinium), Tb, Dy, Ho (holmium), Er (erbium), Tm (thulium), Yb, and Lu. Also measured were Hf, Ta, and Th. All values were reported in parts per million (Appendix F).

Comparison of the NAA, XRF, and ICP-MS data finds excellent agreement throughout. The NAA data cover a wider range of elements than either XRF or ICP-MS. XRF permitted measurement of several elements not possible by NAA, including Mg, Si, Cu, Ga, Y, Nb, and Pb. Although ICP-MS is more laborious, five rare-earth elements (Pr, Gd, Ho, Er, and Tm) not possible by NAA or XRF were also measured. The suites of elements obtained with XRF and ICP-MS are especially useful for geological interpretations and are used accordingly in other chapters of this report. For the purpose of archaeological interpretation, specifically for sourcing artifacts, NAA provides the largest and most precise suite of elements. Thus, we will focus only on the NAA data in the remainder of this chapter.

Quantitative Analysis of the Chemical Data

The NAA analyses at MURR determined concentrations for 33 elements. However, a few elements, especially As, Cr, Ni, and V, were below detection in half or more of the samples. U and Sr were also missing for samples from specific quarries. Treatment of missing values for small groups can be difficult, and as a consequence these six elements were deleted from consideration during statistical analysis. Missing values for the remaining elements were replaced by substituting numbers according to a "best fit" criterion that minimized the Mahalanobis distance of each specimen to the centroid of its quarry zone. Analysis was subsequently carried out on base-10 logarithms of concentrations for the 27 elements that remained. Use of log concentrations instead of raw data compensates for differences in magnitude between major elements such as Fe on one hand and trace elements such as the rare-earth or lanthanide elements on the other. Transformation to base-10 logarithms also yields a more nearly normal distribution for many trace elements.

The primary goal of quantitative analysis of the chemical data is to recognize compositionally homogeneous groups within the analytical database. Based on the "provenance postulate" (Weigand et al. 1977), such groups are assumed to represent geographically restricted sources or source zones. The location of sources or source zones may be inferred by comparing the unknown groups to knowns (source raw materials) or by indirect means. Such indirect means include the "criterion of abundance" (Bishop et al. 1982) or arguments based on geological and sedimentological characteristics (e.g., Steponaitis et al. 1996).

Principal components analysis (PCA) is one of the techniques that can be used to identify patterns (i.e., subgroups) in compositional data. PCA provides new reference axes that are arranged in decreasing order of variance subsumed. The data can be displayed on combinations of these new axes, just as they can be displayed relative to the original elemental concentration axes. PCA can be used in a pure pattern-recognition mode, i.e., to search for subgroups in an undifferentiated data set, or in a more evaluative mode, i.e., to assess the coherence of hypothetical groups suggested by other archaeological criteria. Generally, compositional differences between specimens can be expected to be larger for specimens in different groups than for specimens in the same group, and this implies that groups should be detectable as distinct areas of high point density on plots of the first few components.

One strength of PCA, discussed by Baxter (1992) and Neff (1994), is that it can be applied as a simultaneous R- and Q-mode technique, with both variables (elements) and objects (individual analyzed samples) displayed on the same set of principal component reference axes. The two-dimensional plot of element coordinates on the first two principal components is generally the best possible two-dimensional representation of the correlation or variance-covariance structure in the data: small angles between vectors from the origin to variable coordinates indicate strong positive correlation; angles close to 90^o indicate no correlation; and angles close to 180^o indicate negative correlation. Likewise, the plot of object coordinates is the best two-dimensional representation of Euclidean relations among the objects in log-concentration space (if the PCA was based on the variance-covariance matrix) or standardized log-concentration space (if the PCA was based on the correlation matrix). Displaying objects and variables on the same plots makes it possible to observe the contributions of specific elements to group separation and to the distinctive shapes of the various groups. Such diagrams are often called "biplots" in reference to the simultaneous plotting of objects and variables. The variable interrelationships inferred from a biplot can be verified directly by inspection of bivariate elemental concentration plots (note that a bivariate plot of elemental concentrations is not a biplot).

Whether a group is discriminated easily from other groups can be evaluated visually in two dimensions or statistically in multiple dimensions. A metric known as Mahalanobis distance (or generalized distance) makes it possible to describe the separation between groups or between individual points and groups on multiple dimensions. The Mahalanobis distance of a specimen from a group centroid (Bieber et al. 1976; Bishop and Neff 1989; Neff 2001; Harbottle 1976; Sayre 1975) is:

$$D^2_{y,X} = [y - \overline{X}]^t I_x [y - \overline{X}] \quad (1)$$

where y is $1 \times m$ array of logged elemental concentrations for the individual point of interest, X is the $n \times m$ data matrix of logged concentrations for the group to which the point is being compared with $\overline{X}$ being its $1 \times m$ centroid, and I_x is the inverse of the $m \times m$ variance-covariance matrix of group X. Because Mahalanobis distance takes into account variances and covariances in the multivariate group, it is analogous to expressing distance from a univariate mean in standard deviation units. Like standard deviation units, Mahalanobis distances can be converted into probabilities of group membership for each specimen (e.g., Bieber et al. 1976; Bishop and Neff 1989; Harbottle 1976). For relatively small sample sizes, it is appropriate to base probabilities on Hotelling's T^2, the multivariate extension of the univariate Student's t test.

With small groups, Mahalanobis-distance-based probabilities of group membership may fluctuate dramatically depending on whether or not each specimen is assumed to be a member of the group to which it is being compared. Harbottle (1976) calls this phenomenon "stretchability" in reference to the tendency of an included specimen to stretch the group in the direction of its own location in the elemental concentration space. This problem can be circumvented by cross-validation (or "jackknifing"), that is, by removing each specimen from its presumed group before calculating its own probability of membership (Baxter 1994; Leese and Main 1994). This is a conservative approach to group evaluation that may sometimes exclude true group members. All probabilities discussed below are cross-validated.

In this study, several of the group sizes are smaller than the total number of variates, and this places a further constraint on use of Mahalanobis distance: with more variates than objects, the group variance-covariance matrix is singular, thus rendering calculation of I_x (and D^2 itself) impossible. Dimensionality of the groups therefore must be reduced somehow. One approach to dimensionality reduction would be to eliminate elements considered irrelevant or redundant. The problem with this approach is that the investigator's preconceptions about which elements should best discriminate sources may not be valid; it also squanders one of the major strengths of NAA, namely its capability to determine a large number of elements simultaneously. An alternative approach to dimensionality reduction, used here, is to calculate Mahalanobis distances not with log concentrations but with scores on principal components extracted from the variance-covariance or correlation matrix of the complete data set. This approach entails only the assumption, entirely reasonable in light of the above discussion of PCA, that most group-separating differences should be visible on the largest several components. Unless a data set is highly complex, with numerous distinct groups, using enough components to subsume 90% of total variance in the data may be expected to yield Mahalanobis distances that approximate Mahalanobis distances in the full elemental concentration space.

Results and Conclusions

After eliminating the six elements mentioned earlier (i.e., As, Cr, Ni, Sr, U, and V), the NAA data were converted to logarithms. An RQ-mode PCA transformation of the 80-specimen dataset was performed using the variance-covariance matrix of the logged data (Table 5.1). Based on the calculated eigenvalues, the first seven components subsume at least 90% of the variance in the dataset, and the first 15 components subsume more than 99% of the variance. From the biplots in Figures 5.1 and 5.2 showing the samples and element vectors for the first three principal components, it is noted that the first principal component is dominated by enrichment of the transition metals Co, Fe, Mn, and Ca and dilution of Ta and Th and the alkali elements K and Rb. The second principal component is dominated by enrichment of Ba and dilution of Sb and the rare-earth elements. The third principal component shows enrichment of Na and dilution of K, Rb, Ba, and Cs.

Based on the elemental data and spatial proximity among quarries, the 71 source samples from the Fort Bragg area were subdivided into the eight chemical groups shown in Figures 5.1 and 5.2. The chemical groups are Uwharrie 1, Uwharrie 2, Chatham 1, Chatham 2, Cumberland, Durham, Orange, and Person. Sample FBL039 was removed from the Cumberland group because it was found to be an extreme outlier relative to the five remaining samples. Figures 5.3 through 5.7 illustrate the basic data structure for the analyzed source samples and group

Table 5.1. Principal Components Analysis.[a]

	Principal Components									
	1	2	3	4	5	6	7	8	9	10
La	-0.129	-0.122	-0.017	-0.021	-0.043	-0.012	-0.028	0.001	0.004	0.031
Lu	-0.167	-0.063	0.022	-0.054	0.008	-0.024	0.030	-0.004	0.025	-0.038
Nd	-0.094	-0.149	-0.003	-0.017	-0.009	-0.012	-0.025	0.027	-0.007	0.022
Sm	-0.097	-0.112	-0.006	-0.049	-0.003	-0.026	0.013	0.006	0.007	-0.008
Yb	-0.170	-0.067	0.018	-0.058	0.009	-0.025	0.029	0.003	0.027	-0.035
Ce	-0.126	-0.124	-0.015	-0.012	-0.035	-0.009	-0.017	0.004	0.003	0.018
Co	0.568	-0.141	-0.136	0.097	-0.102	-0.065	-0.013	0.029	0.067	-0.019
Cs	0.005	0.019	-0.274	-0.023	-0.005	-0.003	0.092	0.033	-0.034	0.028
Eu	0.072	-0.006	-0.015	-0.119	-0.075	-0.003	0.034	-0.006	-0.037	0.002
Fe	0.247	-0.108	-0.030	-0.010	0.034	-0.054	0.005	-0.055	-0.001	-0.015
Hf	-0.147	-0.133	0.031	-0.004	-0.018	0.006	-0.025	-0.016	-0.023	-0.035
Rb	-0.233	0.011	-0.242	-0.011	0.109	-0.062	-0.008	0.006	0.008	-0.015
Sb	0.051	-0.177	-0.079	0.091	0.032	0.182	0.074	-0.038	0.000	0.017
Sc	0.224	0.063	-0.057	-0.091	-0.045	0.016	0.061	-0.027	-0.001	-0.036
Ta	-0.249	-0.113	-0.053	0.022	-0.044	0.003	-0.006	0.016	0.013	0.012
Tb	-0.130	-0.090	-0.001	-0.063	0.025	-0.026	0.041	0.000	0.013	-0.023
Th	-0.319	-0.086	-0.063	0.003	-0.112	0.019	-0.021	0.026	-0.021	0.017
Zn	0.126	-0.101	-0.042	0.016	0.017	-0.075	0.032	-0.059	-0.004	0.031
Zr	-0.148	-0.150	0.021	-0.003	-0.038	0.018	-0.036	-0.026	-0.034	-0.023
Al	0.054	-0.016	-0.006	-0.009	0.003	0.007	-0.015	-0.011	0.010	-0.008
Ba	-0.022	0.182	-0.207	-0.084	-0.107	0.055	-0.056	-0.038	0.010	-0.019
Ca	0.352	-0.120	-0.022	-0.153	0.084	0.104	-0.065	0.056	0.034	-0.003
Dy	-0.162	-0.093	-0.002	-0.058	0.019	-0.019	0.036	0.008	0.016	-0.026
K	-0.206	0.008	-0.202	0.054	0.062	0.013	-0.078	-0.059	0.017	-0.022
Mn	0.211	-0.064	-0.004	-0.102	0.026	-0.040	-0.038	-0.057	-0.030	0.082
Na	0.010	-0.025	0.110	-0.014	-0.045	0.024	0.011	-0.078	0.027	-0.030
Ti	0.285	-0.076	-0.034	0.039	0.019	-0.011	-0.030	0.021	-0.115	-0.068
Eigenvalue	1.123	0.282	0.269	0.102	0.091	0.074	0.050	0.037	0.029	0.023
Variance (%)	51.6	12.9	12.4	4.7	4.2	3.4	2.3	1.7	1.3	1.1
Cumulative (%)	51.6	64.6	76.9	81.6	85.8	89.2	91.5	93.2	94.5	95.6

[a] Based on variance-covariance matrix for all 80 samples (FBL001-FBL080).

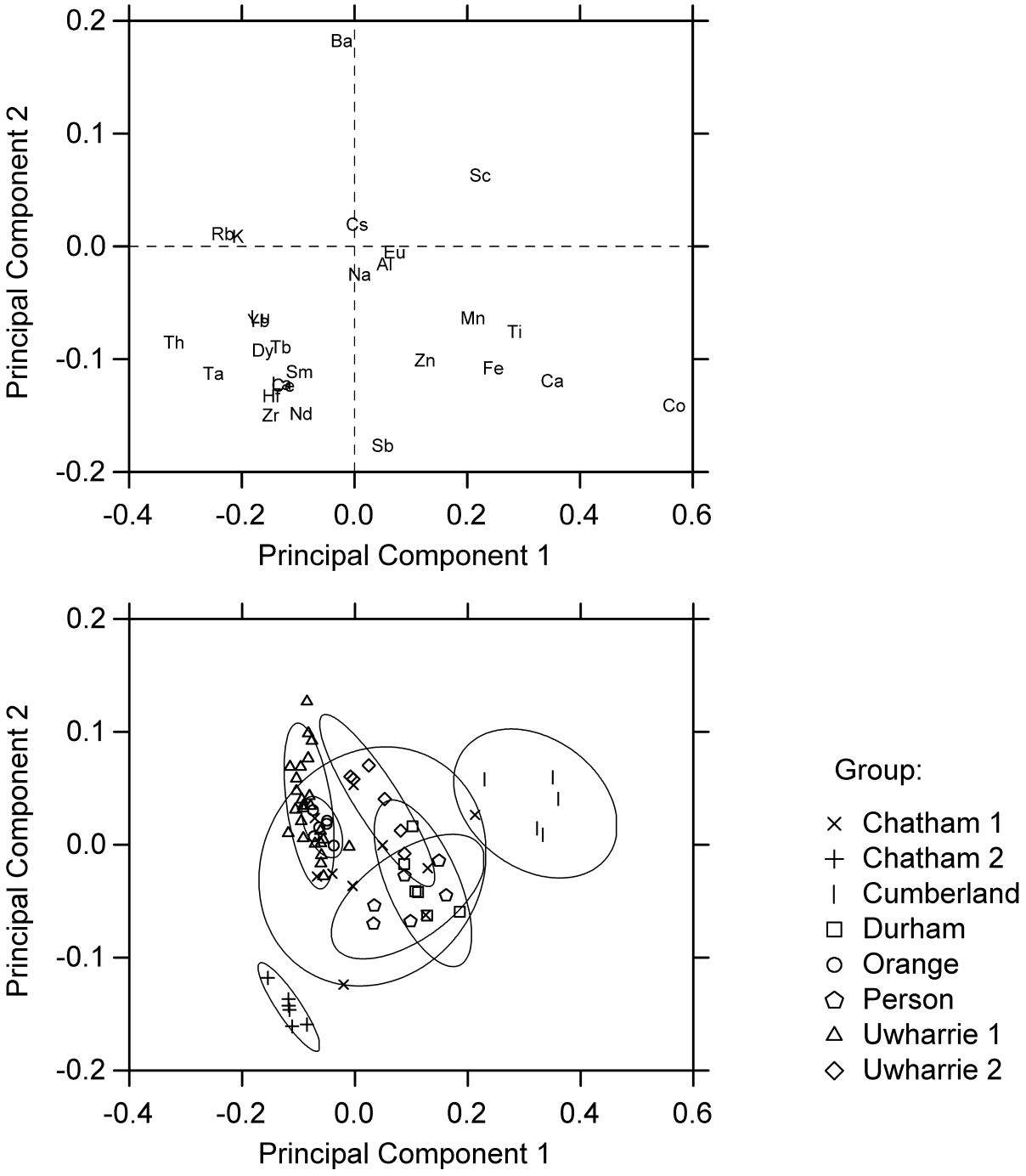

Figure 5.1. Biplot derived from PCA of the variance-covariance matrix of the NAA data showing principal component 1 versus principal component 2. Elements are shown in the top graph; analyzed specimens are shown in the bottom graph. Ellipses represent 90% confidence level for membership in the groups.

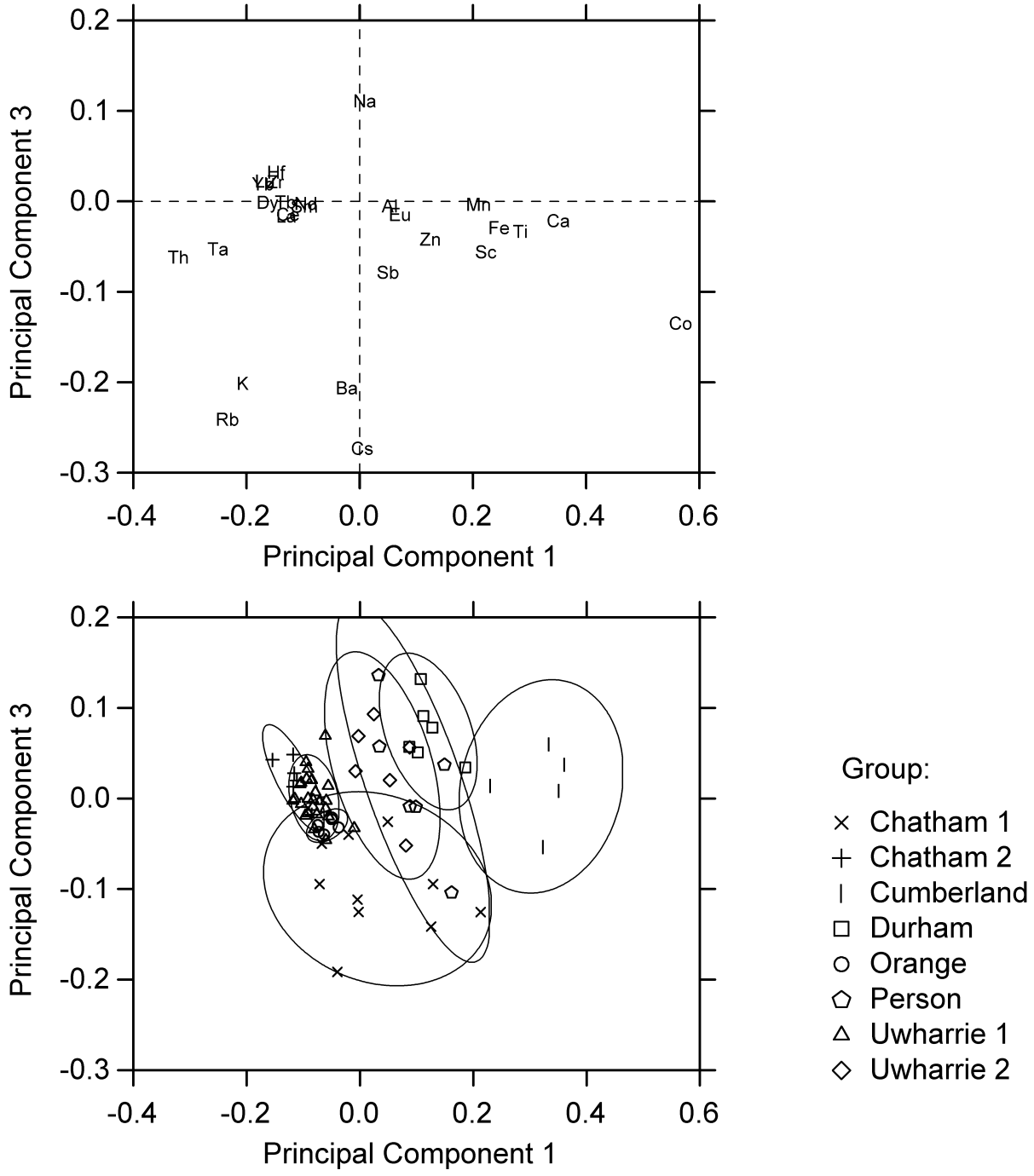

Figure 5.2. Biplot derived from PCA of the variance-covariance matrix of the NAA data showing principal component 3 versus principal component 1. Elements are shown in the top graph; analyzed specimens are shown in the bottom graph. Ellipses represent 90% confidence level for membership in the groups.

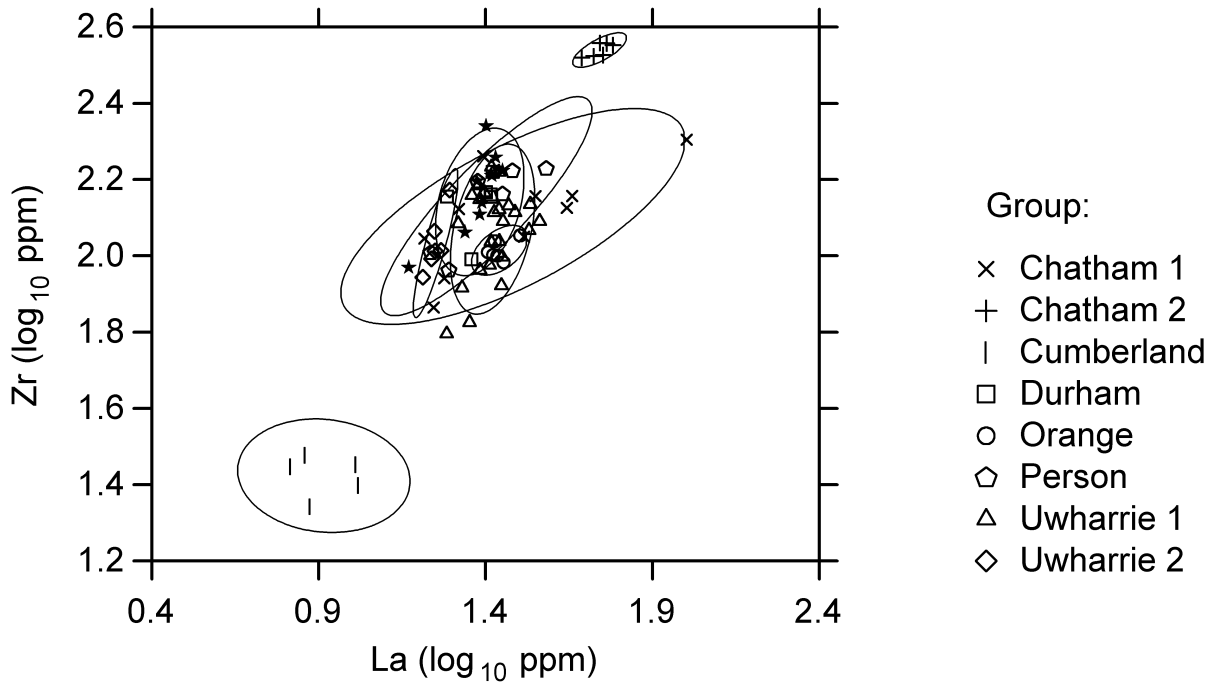

Figure 5.3. Bivariate plot of Zr versus La for the chemical groups. Ellipses represent 90% confidence level for membership in the groups. Artifacts are plotted as solid stars.

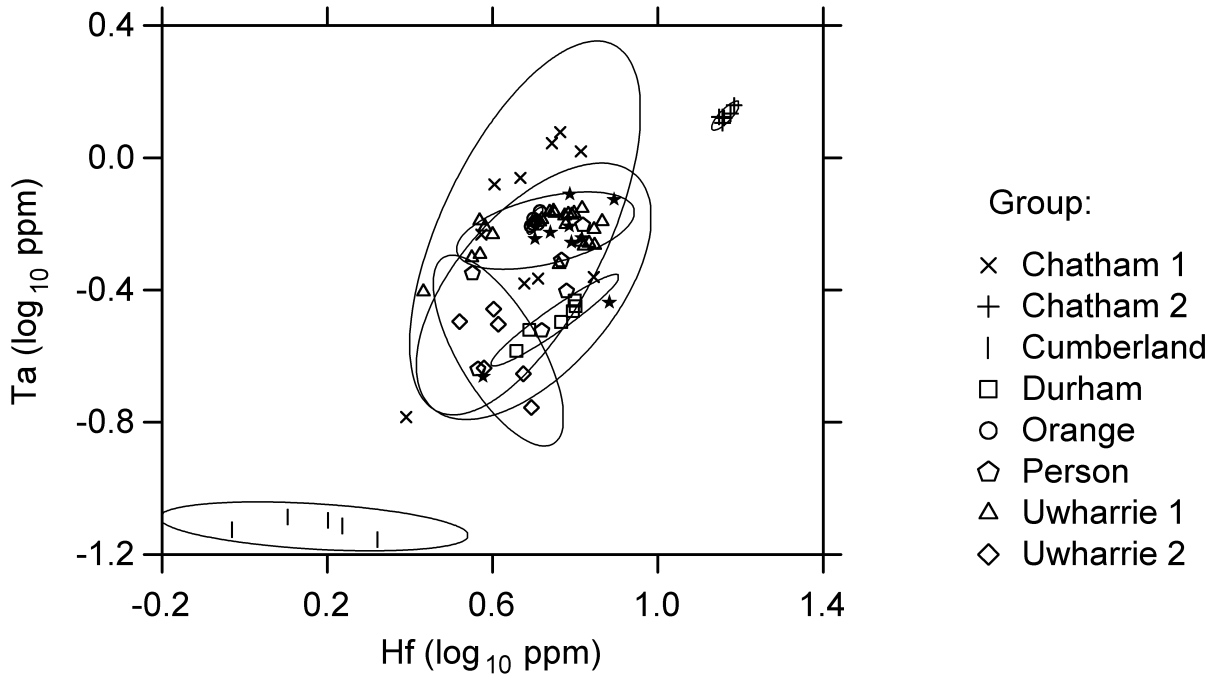

Figure 5.4. Bivariate plot of Ta versus Hf for the chemical groups. Ellipses represent 90% confidence level for membership in the groups. Artifacts are plotted as solid stars.

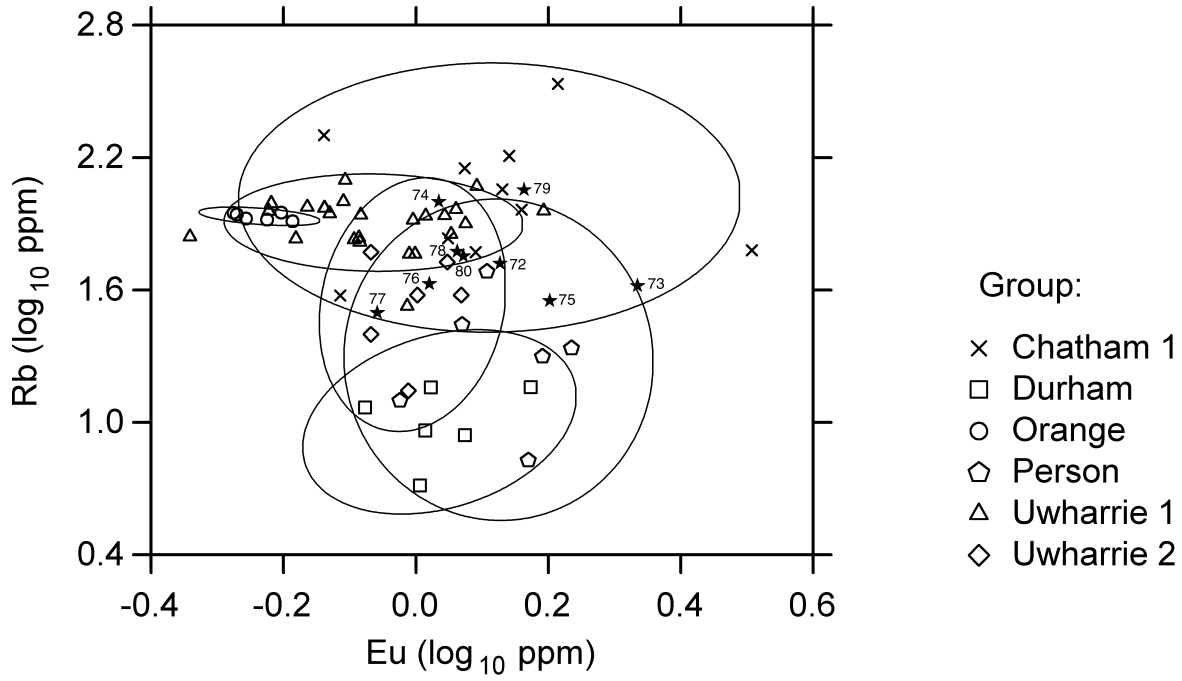

Figure 5.5. Bivariate plot of Rb versus Eu for six of the chemical groups. Ellipses represent 90% confidence level for membership in the groups. Artifacts are plotted as solid stars; individual artifacts are labeled with their FBL-number suffixes.

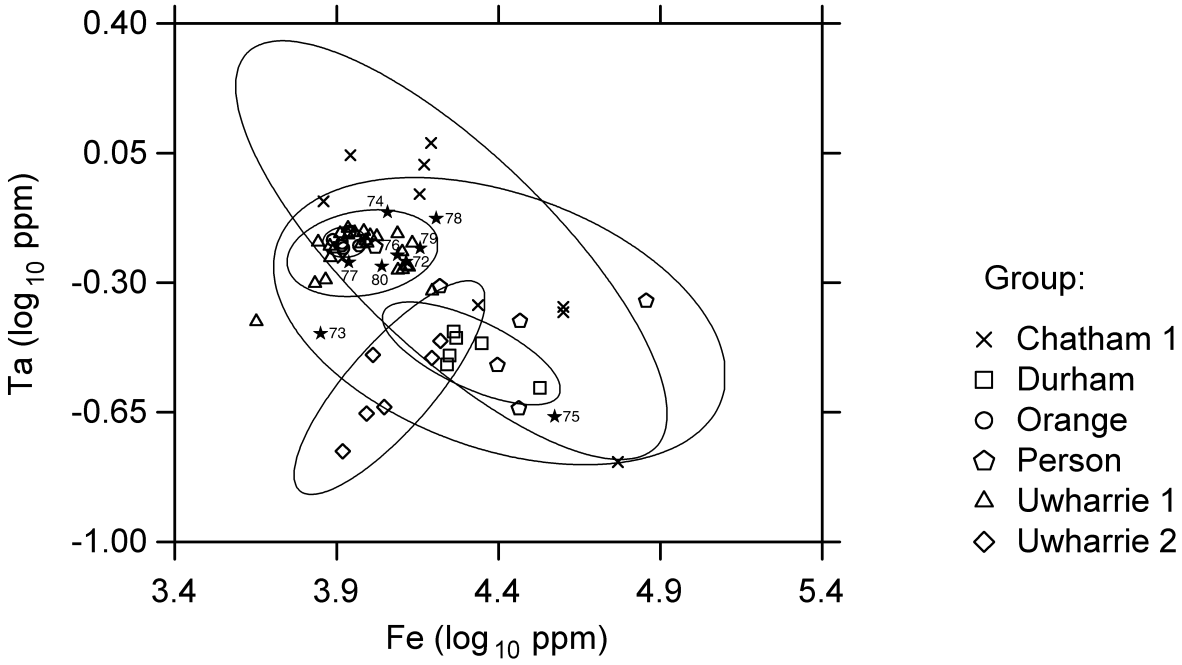

Figure 5.6. Bivariate plot of Ta versus Fe for six of the chemical groups. Ellipses represent 90% confidence level for membership in the groups. Artifacts are plotted as solid stars; individual artifacts are labeled with their FBL-number suffixes.

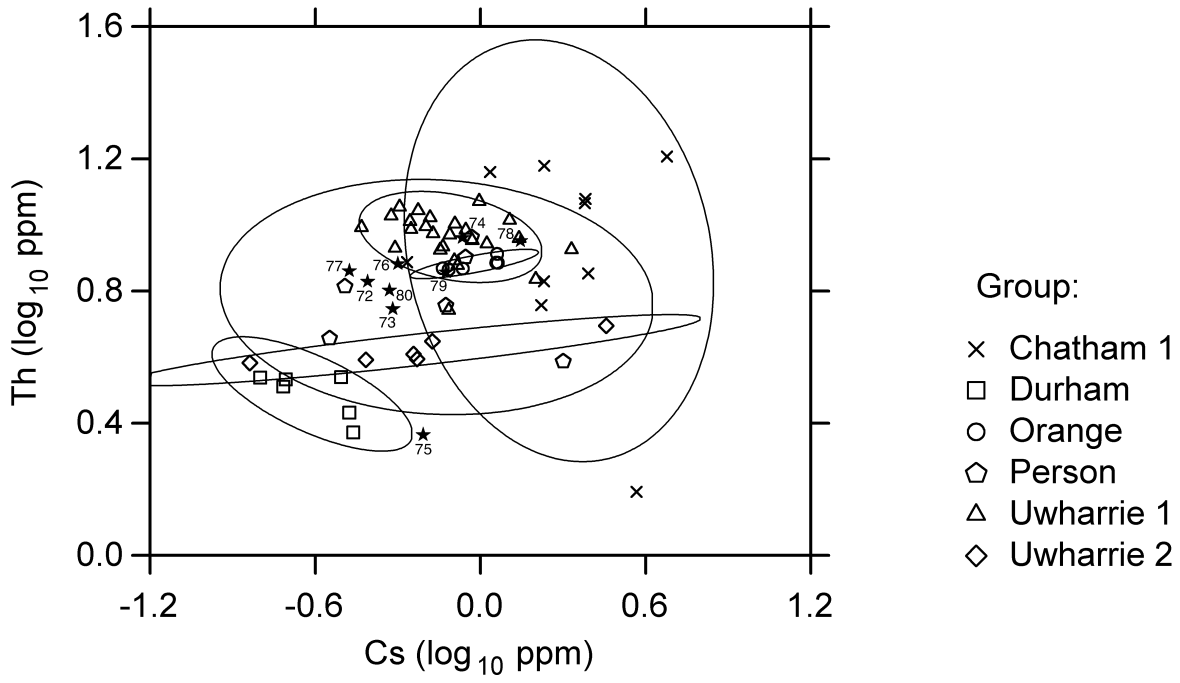

Figure 5.7. Bivariate plot of Th versus Cs for six of the chemical groups. Ellipses represent 90% confidence level for membership in the groups. Artifacts are plotted as solid stars; individual artifacts are labeled with their FBL-number suffixes.

assignments and also show the artifact data projected against the source groups. Table 5.2 lists the means and standard deviations for each of the compositional groups based on NAA data.

The Uwharrie 1 group is statistically the most valid of the groups, a consequence of the number of samples having membership in the group. Additional analyses of source specimens from this quarry would not be likely to affect the overall basic structure of this group. According to Mahalanobis distance calculations for samples in the Uwharrie 1 group, membership probabilities based on the first 15 principal components are greater than 1% for all members of this group (except FBL013 and FBL014). The results are shown in Table 5.3.

A comparison of specimens from the other compositional groups to Uwharrie 1 illustrates that with the exception of the Orange group all other chemical groups have low probabilities of overlap with Uwharrie 1 (Table 5.3). Due to the limited numbers of samples in the individual groups (ranging from 5 to 10 samples), we are unable to perform the same test to differentiate between the other quarries.

As shown in Figures 5.3 and 5.4, the rock specimens exhibit some significant patterns in geochemistry. Three distinct clusters are present, with the Chatham 2 and Cumberland groups well separated from the remaining compositional groups on the basis of Hf, Ta, and Zr. The Chatham 2 source samples are an intermediate metavolcanic rock, and the Cumberland specimens are largely greenstone. Both groups are small but compositionally very homogeneous. Although it is unlikely that additional samples from these quarries would have much effect on the basic structure of the database, the analysis of additional specimens would enable more rigorous testing.

Table 5.2. Element Means and Standard Deviations Within Chemical Groups.

Element	Uwharrie 1 (n = 25)	Uwharrie 2 (n = 6)	Chatham 1 (n = 10)	Chatham 2 (n = 6)	Cumberland (n = 5)	Durham (n = 6)	Orange (n = 6)	Person (n = 6)
La (ppm)	26.7 ± 4.2	17.8 ± 1.1	35.7 ± 25.2	55.4 ± 4.1	8.4 ± 1.8	24.3 ± 2.8	27.7 ± 2.2	26.2 ± 7.7
Lu (ppm)	0.858 ± 0.239	0.564 ± 0.137	0.566 ± 0.269	1.152 ± 0.059	0.249 ± 0.089	0.446 ± 0.038	0.661 ± 0.07	0.507 ± 0.158
Nd (ppm)	24.2 ± 4.2	19.0 ± 3.2	35.6 ± 22.1	73.3 ± 20.6	12.5 ± 3.8	27.6 ± 7.6	33.3 ± 4.6	30.2 ± 9.4
Sm (ppm)	6.64 ± 1.67	4.76 ± 0.59	7.46 ± 3.97	12.73 ± 0.71	3.48 ± 1.37	5.06 ± 0.56	6.42 ± 0.60	6.04 ± 1.54
Yb (ppm)	5.78 ± 1.63	3.72 ± 0.82	4.04 ± 1.97	7.99 ± 0.34	1.73 ± 0.62	2.95 ± 0.23	4.50 ± 0.45	3.18 ± 1.05
Ce (ppm)	56.5 ± 9.3	37.8 ± 3.1	70.6 ± 34.0	124.1 ± 6.6	19.6 ± 5.5	52.4 ± 6.2	61.2 ± 5.6	56.9 ± 12.6
Co (ppm)	0.43 ± 0.16	1.44 ± 1.15	6.36 ± 6.99	0.70 ± 0.49	24.84 ± 9.82	5.03 ± 2.95	0.67 ± 0.18	6.88 ± 7.69
Cs (ppm)	0.85 ± 0.40	0.87 ± 0.99	2.24 ± 1.23	0.45 ± 0.12	0.78 ± 0.40	0.27 ± 0.09	0.97 ± 0.20	0.86 ± 0.62
Eu (ppm)	0.895 ± 0.246	0.996 ± 0.13	1.406 ± 0.696	0.43 ± 0.052	1.163 ± 0.371	1.103 ± 0.22	0.582 ± 0.05	1.358 ± 0.28
Fe (ppm)	9909 ± 2676	11963 ± 3370	22910 ± 17360	19008 ± 968	72284 ± 11336	21339 ± 6321	8432 ± 540	30334 ± 21627
Hf (ppm)	5.51 ± 1.27	4.15 ± 0.60	4.96 ± 1.35	14.59 ± 0.46	1.53 ± 0.44	5.69 ± 0.78	5.05 ± 0.10	5.15 ± 1.27
Rb (ppm)	82.9 ± 19.6	37.9 ± 16.9	127.8 ± 91.2	115.9 ± 21.5	23.8 ± 11.8	11.0 ± 3.9	85.9 ± 3.3	22.9 ± 14.5
Sb (ppm)	0.172 ± 0.139	0.145 ± 0.087	0.312 ± 0.22	0.49 ± 0.163	0.397 ± 0.592	0.331 ± 0.135	0.307 ± 0.076	0.444 ± 0.123
Sc (ppm)	5.83 ± 1.73	7.70 ± 2.47	9.90 ± 4.52	1.70 ± 0.40	26.93 ± 10.35	8.17 ± 2.60	5.31 ± 0.42	12.87 ± 10.85
Ta (ppm)	0.608 ± 0.079	0.269 ± 0.068	0.709 ± 0.35	1.342 ± 0.056	0.077 ± 0.005	0.325 ± 0.04	0.645 ± 0.025	0.415 ± 0.141
Tb (ppm)	1.119 ± 0.293	0.751 ± 0.088	0.99 ± 0.565	1.911 ± 0.131	0.532 ± 0.264	0.614 ± 0.082	1.1 ± 0.101	0.789 ± 0.215
Th (ppm)	9.31 ± 1.43	4.20 ± 0.44	9.83 ± 4.75	12.78 ± 0.46	0.53 ± 0.37	3.11 ± 0.47	7.62 ± 0.32	6.32 ± 2.04
Zn (ppm)	39.7 ± 13.7	40.1 ± 15.2	58.9 ± 21.3	77.0 ± 27.6	100.8 ± 27.1	54.2 ± 13.2	33.4 ± 7.0	97.0 ± 84.3
Zr (ppm)	121.4 ± 29.8	109.6 ± 21.3	132.2 ± 39.4	346.8 ± 14.5	26.7 ± 3.2	140.2 ± 22.5	103.6 ± 6.3	138.8 ± 33.7
Al (ppm)	55640 ± 5324	57312 ± 5749	68527 ± 12938	61232 ± 2284	92072 ± 6069	75798 ± 7137	64847 ± 2936	66258 ± 11079
Ba (ppm)	511 ± 127	340 ± 88	1026 ± 515	67 ± 8	246 ± 49	314 ± 156	694 ± 74	367 ± 241
Ca (ppm)	2843 ± 1643	9534 ± 4486	9969 ± 9902	4186 ± 1483	50932 ± 24188	13940 ± 7499	4862 ± 558	8128 ± 4617
Dy (ppm)	6.53 ± 1.69	4.00 ± 0.29	5.84 ± 3.28	11.57 ± 0.31	2.40 ± 1.18	3.46 ± 0.38	6.38 ± 0.68	4.31 ± 1.61
K (ppm)	23411 ± 6230	13532 ± 3766	36108 ± 15997	35210 ± 6863	6864 ± 5154	7764 ± 2671	30612 ± 2411	10122 ± 8068
Mn (ppm)	324 ± 106	605 ± 87	679 ± 366	413 ± 88	1588 ± 331	750 ± 170	263 ± 69	555 ± 157
Na (ppm)	25864 ± 3909	27432 ± 5168	20559 ± 13100	26636 ± 4362	25145 ± 11777	42853 ± 4957	27469 ± 2554	36661 ± 5724
Ti (ppm)	616 ± 309	1068 ± 273	1862 ± 1198	976 ± 194	4933 ± 1790	2062 ± 890	757 ± 151	2046 ± 590

Table 5.3. Rock Samples Arranged by Chemical Group, With Mahalanobis Probabilities of Membership in the Uwharrie 1 Group.

Chemical Group: Sample	Quarry Zone	Field Name	Normative Name	TAS Name	Probability of Membership in Uwharrie 1
Cumberland:					
FBL040	Cumberland County	basalt	andesite/basalt	basaltic trachyandesite	0.000
FBL041	Cumberland County	diorite	andesite/basalt	basaltic trachyandesite	0.000
FBL042	Cumberland County	tuff?	andesite/basalt	trachybasalt	0.000
FBL070	Cumberland County	greenstone	andesite/basalt	basalt	0.000
FBL071	Cumberland County	metagabbro	andesite/basalt	basalt	0.000
Chatham 1:					
FBL027	Chatham Pittsboro	mudstone	rhyodacite	-	0.177
FBL028	Chatham Pittsboro	mudstone	alkali feldspar rhyolite	rhyolite	0.000
FBL029	Chatham Pittsboro	siltstone	rhyodacite	rhyolite	0.016
FBL030	Chatham Pittsboro	fine sandstone	dacite	rhyolite	0.001
FBL035	Chatham Siler City	mud/siltstone	dacite	dacite	0.035
FBL036	Chatham Siler City	dacite	andesite/basalt	rhyolite	0.039
FBL037	Chatham Siler City	mudstone	rhyodacite	dacite	0.005
FBL038	Chatham Siler City	sandstone	andesite/basalt	trachyandesite	0.001
FBL056	Chatham Pittsboro	mudstone	alkali feldspar rhyolite	-	0.009
FBL057	Chatham Pittsboro	mudstone	dacite	rhyolite	0.155
Chatham 2:					
FBL031	Chatham Silk Hope	dacite/rhyodacite	rhyodacite	rhyolite	0.000
FBL032	Chatham Silk Hope	lithic tuff	dacite	rhyolite	0.000
FBL033	Chatham Silk Hope	dacite	rhyodacite	rhyolite	0.000
FBL034	Chatham Silk Hope	lithic tuff	dacite/rhyodacite	rhyolite	0.000
FBL058	Chatham Silk Hope	lithic tuff	rhyodacite	rhyolite	0.000
FBL059	Chatham Silk Hope	lithic tuff	rhyodacite	rhyolite	0.000
Durham:					
FBL047	Durham County	dacite	dacite	rhyolite	0.017
FBL048	Durham County	sandstone	andesite/basalt	trachyte	0.026
FBL049	Durham County	sandstone	andesite/basalt	rhyolite	0.084
FBL050	Durham County	tuff	andesite/basalt	rhyolite	0.032
FBL066	Durham County	dacite	andesite/basalt	rhyolite	0.041
FBL067	Durham County	sandstone	andesite/basalt	trachydacite	0.016
Orange:					
FBL060	Orange County	dacite	dacite	rhyolite	45.135
FBL061	Orange County	dacite	dacite	rhyolite	42.825
FBL062	Orange County	dacite	dacite	rhyolite	51.821
FBL063	Orange County	dacite	dacite	rhyolite	63.075
FBL064	Orange County	dacite	rhyodacite	rhyolite	74.721
FBL065	Orange County	dacite	dacite	rhyolite	80.739
Person:					
FBL043	Person County	mudstone?	andesite/basalt	trachyte	0.009
FBL044	Person County	tuff	dacite	rhyolite	1.518
FBL045	Person County	mudstone	andesite/basalt	rhyolite	0.020
FBL046	Person County	sandstone	dacite	rhyolite	0.025
FBL068	Person County	siltstone	dacite	rhyolite	0.032
FBL069	Person County	siltstone	dacite	rhyolite	0.012

Table 5.3. Rock Samples Arranged by Chemical Group, With Mahalanobis Probabilities of Membership in the Uwharrie 1 Group (continued).

Chemical Group: Sample	Quarry Zone	Field Name	Normative Name	TAS Name	Probability of Membership in Uwharrie 1
Uwharrie 1:					
FBL001	Uwharries Eastern	dacite	dacite	rhyolite	16.259
FBL002	Uwharries Eastern	dacite	dacite	rhyolite	55.101
FBL003	Uwharries Eastern	dacite	dacite/rhyodacite	rhyolite	20.157
FBL004	Uwharries Eastern	dacite	dacite	rhyolite	4.879
FBL005	Uwharries Eastern	dacite	dacite	rhyolite	1.858
FBL006	Uwharries Eastern	dacite	dacite	rhyolite	90.923
FBL007	Uwharries Eastern	dacite	rhyodacite	rhyolite	34.740
FBL008	Uwharries Western	andesite	dacite	rhyolite	86.592
FBL009	Uwharries Western	andesite	dacite	rhyolite	45.329
FBL010	Uwharries Western	andesite	dacite	rhyolite	12.279
FBL011	Uwharries Western	andesite	dacite	rhyolite	94.411
FBL012	Uwharries Western	andesite/latite	dacite	rhyolite	94.736
FBL013	Uwharries Western	andesite	dacite	rhyolite	0.231
FBL014	Uwharries Western	andesite/latite	dacite	rhyolite	0.612
FBL015	Uwharries Southern	felsite	dacite	rhyolite	84.734
FBL016	Uwharries Southern	felsite	dacite	rhyolite	64.795
FBL017	Uwharries Southern	felsite	dacite	rhyolite	63.901
FBL018	Uwharries Southern	felsite	dacite	rhyolite	66.801
FBL019	Uwharries Southern	felsite	dacite	rhyolite	89.434
FBL025	Uwharries Southeastern	dacite	rhyodacite	rhyolite	87.153
FBL026	Uwharries Southeastern	dacite	dacite	rhyolite	37.897
FBL051	Uwharries Southeastern	dacite	rhyodacite	-	95.755
FBL052	Uwharries Southeastern	dacite	-	-	3.543
FBL053	Uwharries Southeastern	dacite	dacite	rhyolite	79.296
FBL054	Uwharries Southeastern	dacite	rhyodacite	-	56.695
Uwharrie 2:					
FBL020	Uwharries Asheboro	tuff	dacite	rhyolite	0.404
FBL021	Uwharries Asheboro	dacite/andesite	dacite	rhyolite	0.138
FBL022	Uwharries Asheboro	dacite/andesite	dacite	rhyolite	0.587
FBL023	Uwharries Asheboro	dacite	dacite	rhyolite	0.045
FBL024	Uwharries Asheboro	tuff	dacite	rhyolite	0.991
FBL055	Uwharries Asheboro	dacite	dacite	rhyolite	1.164
Ungrouped:					
FBL039	Cumberland County	aplite	rhyodacite	rhyolite	

From Figures 5.3 and 5.4, it is obvious that both Chatham 2 and Cumberland can be excluded as possible sources for the nine artifacts in this study. In Figures 5.5 through 5.7, the artifacts are projected against the remaining six chemical groups. Examination of the plots suggests that Uwharrie 1 is the most probable source for all of the artifacts except FBL073 and FBL075. The latter two artifacts have greater likelihood of belonging to the Chatham 1 or Person sources. We support this observation by calculating the Mahalanobis distance probabilities where the probabilities of the artifacts relative to the Uwharrie 1 source were determined using 99% of the variance in the database (Table 5.4). Probabilities are high for FBL074, FBL076, and FBL077 to belong to the Uwharrie 1 group. Samples FBL072, FBL078, FBL079, and FBL080 have modest probabilities of membership. The extremely low probabilities for FBL073 and FBL075 suggest they are from a different source.

Table 5.4. Fort Bragg Artifacts, With Mahalanobis Probabilities of Membership in the Uwharrie 1 Group.

Sample	Site	Field Name	Normative Name	TAS Name	Probability of Membership in Uwharrie 1
FBL072	31Hk100	dacite	dacite	rhyolite	3.287
FBL073	31Hk148	dacite	dacite	rhyolite	0.006
FBL074	31Hk173	dacite	dacite	rhyolite	27.184
FBL075	31Hk182	andesite	andesite/basalt	dacite	0.041
FBL076	31Hk224	tuff/siltstone	dacite	rhyolite	37.415
FBL077	31Hk737	siltstone	dacite	rhyolite	20.243
FBL078	31Hk999	dacite	dacite	rhyolite	1.536
FBL079	31Hk1408	dacite	dacite	rhyolite	5.457
FBL080	Flat Creek	dacite	dacite	rhyolite	1.163

Acknowledgments

We thank Kyra Lienhop and Nicole Little for carrying out the NAA sample preparation and measurements, Derek Carson for carrying out the XRF sample preparation and measurements, and Pamela Altman and James Guthrie for carrying out the sample digestions and sample measurements by ICP-MS.